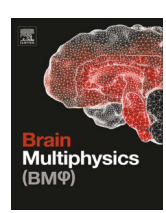
ELSEVIER

Contents lists available at ScienceDirect

# **Brain Multiphysics**

journal homepage: www.sciencedirect.com/journal/brain-multiphysics



# Comprehensive study of sex-based anatomical variations of human brain and development of sex-specific brain templates

Mohammadreza Ramzanpour<sup>a</sup>, Bahram Jafari<sup>a</sup>, Jeremy Smith<sup>b</sup>, Jason Allen<sup>b</sup>, Marzieh Hajiaghamemar<sup>a,\*</sup>

#### ARTICLE INFO

Keywords: Human brain Sex-based brain structural variations Sex-specific brain template Traumatic brain injury

# ABSTRACT

The sex-based human brain structural variations alongside the necessity and development process for sex-specific brain templates were investigated in this study. Comparing magnetic resonance images of 500 female and 500 male subjects, no significant sex-based difference was observed for average cortical thickness, however, all the volumetric values, including the total brain volume (TBV) and major 19 brain regions, were found to be significantly different between females and males. Moreover, analyzing the fractional volume of the regions showed that these sex variations were not proportional to TBV for all regions. These findings underscore the importance of distinguishing the sex-based differences in human brain studies. While brain templates have been developed for general population and cohorts with the same characteristics such as race or age, there is a lack of sex-specific brain templates. To fill this gap and find a representative reference brain image for each sex, nonlinear templates were developed for female, male, and mixed population subjects. Next, a separate set of 109 female and 109 male brain images were used to evaluate the sex-specificity of the brain templates. It was observed that the female and male test subjects were registered to their sex-specific templates with the lowest amount of deformation/warping confirming better representativeness of the sex-specific templates for their target population. The findings of this study including the templates and the reported variations can be used in research involving sex dimorphic brain disorders, diseases, and/or injuries such as traumatic brain injury that is affected by the sex-based brain anatomical differences.

Statement of significance: Human brain exhibits sex-based variation both in size and volumetric composition of different regions. Despite these differences, there is a paucity of sex-specific brain templates. Addressing this gap marks the significance of our study as briefly explained here. We have shown that differences in male and female brain go beyond simple scaling and the observation of regional differences that are not proportional to the sex-based total brain volume variations has motivated us to develop sex-specific templates. The representativeness and difference of these sex-specific templates were assessed by measuring the amount of required warping in nonlinear registration of test subjects to them. It was shown that registration of female and male subjects to their corresponding sex-specific template involved lower level of warping compared to their registration to their opposite sex or mixed population brain template.

# Introduction

Human brain is known to have differences based on sex, and its related diseases, disorders, and injuries such as autism, depression, Alzheimer's disease, and traumatic brain injury (TBI) [1] also exhibit sex differences in prevalence, onset, and outcomes. The brain sex differences can be divided into structural, chemical, and functional [2,3]

which can contribute to the variations observed in different brain related health conditions. However, the structural differences are the ones that can be computationally and biomechanically modeled and are believed to affect or be directly affected by different brain-related diseases, disorders, or injuries [4,5]. For example, brain structural differences have shown to be effective on TBI [6], which is the leading cause of cognitive and behavioral deficits worldwide with ~50 million

E-mail address: marzieh.memar@utsa.edu (M. Hajiaghamemar).

https://doi.org/10.1016/j.brain.2023.100077

<sup>&</sup>lt;sup>a</sup> Department of Biomedical Engineering and Chemical Engineering, The University of Texas at San Antonio, San Antonio, TX, United States

b Department of Radiology and Imaging Sciences, Emory University School of Medicine, Atlanta, GA, United States

<sup>\*</sup> Corresponding author.

occurrences and  $\sim$ \$400 billion cost annually [7]. The structural variation study of the human brain is especially important from biomechanical point of view due to the widespread use of numerical finite element models (FEM) of brain in the study of TBI and the fact that structural variations affect the responses of brain FEMs [8]. In the following sections, we will review some of the studies corroborating sex-based structural differences, the existing brain templates/atlases, and current sex-specific needs and gaps in the brain related fields, especially TBI and brain FEM in which the sex variation is an important factor.

# Sex-based structural differences in human brain

Studies have shown that structural differences exist between male and female brain [9 12]. The total brain volume (TBV) is the most observable sexually dimorphic feature in the brain, with reported larger average value for men than for women [13]. Sex variations were also observed in different brain regions and sub-regions. For example, Ruigrok et al. [12] performed foci-based meta-analyses on regional differences between female and male brains using data from 126 published articles with the subject ages ranging from 10 to 80 years. They found that, in general, men have larger absolute volume in different regions of the brain, ranging from 8% to 13%, with the highest differences in cerebrum and intracranial volume. Another study reported that the gray matter (GM), white matter (WM), and cerebrospinal fluid (CSF) relative volume varies by sex, with men having higher percentage of WM and CSF compared to women, while women have higher percentage of GM [10]. Sub-regional meta-analyses have also revealed sex variations in many sub-regions of brain. For example, it has been reported that males have larger GM volume in the bilateral amygdala, hippocampi, anterior para-hippocampal gyri, posterior cingulate gyri, precuneus, and temporal poles, while females have higher GM volume and thicker gray matter in the parietal lobe, and higher left frontal pole GM tissue density compared to male subjects [10]. These studies suggest that the regional and sub-regional volumetric variations exist between female and male brains, and the variations are not always proportional to the differences in TBV between them. This calls for TBV-normalized volumetric studies to be conducted for better evaluation of sex variations in human brain. However, previous studies on this topic are mainly focused on absolute volumes of brain regions [10 14]. To the best of our knowledge, the closest study that looked at the fractional regional brain volumes was conducted using 23 female and 23 male brain images and reported that the proportional size of many regions with respect to the total hemispheric volume are equal [15]. More studies with larger datasets need to be conducted to elucidate the sex variations in the fractional brain volumes.

Furthermore, although previous studies have provided evidence for sex variations in brain structures [10 14], those studies have several limitations, such as small sample size, wide age range, and differences in the analysis techniques. The latter is especially a limitation with meta-analysis studies and has shown to affect study outcomes. For example, a study published by Tustison et al. [16], found that the cortical thickness estimates, derived from several publicly available datasets, differed markedly when FreeSurfer [17] or ANT [18] software were used. The limitations with previous studies on brain sex variations call for a more comprehensive study to be conducted on a larger dataset, narrower age range, and with more consistent analysis techniques to minimize any biases or misidentifications of sex variations in the brain. In addition, exploring both the absolute and TBV-normalized volumes of the brain regions and sub-regions between females and males on a large dataset will advance the sex-specific knowledge in brain-related fields. Such an exploration and comprehensive brain structural sex variation study is one of the aims of this paper.

#### Human brain templates

As mentioned before, the human brain shows variability among different groups based on age and sex. Therefore, any attempt at grouplevel analysis requires an anatomical reference image, often referred to as an atlas or template, which is representative of that group. Several standardized three-dimensional atlases and templates are commonly used for subject-specific and population-based analysis and comparison of imaging data. Talairach and Tournoux developed the first brain template from a female postmortem subject [19]. There are several other brain templates currently available that are population-based, but they are all developed using mixed-sex data [20 23]. Among those brain templates, the ICBM152, which is developed by the International Consortium of Brain Mapping (ICBM) is one of the most commonly used templates [20]. ICBM152 is the average of co-aligned 152 Magnetic resonance imaging (MRI) scans of mixed-sex subjects aged 18 to 90 years developed with a focus on the relationship between brain microand macroscopic structure and function. ICBM152 is developed for applications in neuroscience and clinical diagnosis. Another population-based template is the Human Connectome Project tractography template (HCP), which is the average of 842 mixed-sex subjects aged 22 to 37 years and developed focusing on structural and functional brain connectivity [21]. Other major population-based templates are Human-Brain-Project [22] and CONNECT [23]. These are also mixed-sex brain templates. Among the current brain templates, Talairach and ICBM152 are used in many software packages, including Free-Surfer and Statistical Parametric Mapping (SPM), for different analysis purposes.

However, the study of brain images within a specific group different from the group used in the development of these common brain templates, requires creating a study-specific template. To this end, there are some age-based ([24,25]) and race-specific templates such as the Chinese [26] and Indian brain templates [27] that have been developed over the years. Moreover, brain templates have been generated for different animals such as ferret [28] and macaque [29]. However, in spite of the sex-based structural differences that observed in human brains, there is a lack of sex-specific human brain templates in the literature. This paucity causes problems for group-level analyses focusing on sex-specific features of the brain and/or brain-related diseases or injury. For example, in the TBI field, such brain templates can be used for development of sex-specific human head FEM to better study the sex variations in the brain tissue s biomechanical responses to impact/trauma events. Moreover, since the group-based brain template can be viewed as the population-based average and representative of that group, it can be used as the 50th percentile of either female or male subjects. However, the paucity of sex-specific brain templates hinders the female- and/or male-focused brain analysis and development of female and male brain FEM. This gap motivated us to fulfill another objective of this study which was to develop sex-based brain templates and to identify the potential differences in those templates.

# Sex variations in TBI and its importance in brain FEM for modeling of TBI

The sex-specific brain knowledge and templates that will be provided in this study can be used in different sex-dimorphic brain-related conditions that are affected by brain structural variations. For example, as mentioned previously, TBI is one of the fields that are affected by the sex variations in the brain and will be discussed further in this paper. While it has been known that the occurrence rate and severity of post-TBI outcomes differ between sexes and females are at higher risk of sustaining concussion/TBI and worse long-term outcomes [30 36], there are not yet sufficient studies to elucidate the factors contributing to these sex differences and how we can intervene. Brain FEM, which can provide insights into tissue responses during biomechanical events, are among the tools that can play an important role in elucidating these sex differences and the factors affecting brain biomechanical responses in

trauma events. Brain FEMs have been used in variety of applications, including TBI prediction [37 40], tissue injury threshold assessment [40 43], and protective headgear development [44 46].

To provide realistic results with the FEM simulations, brain FEMs must be accurate in several aspects including, among others, incorporation of representative volumes and geometrical shapes and inclusion of different components and anatomical features. The importance of size and volumetric parameters on the brain responses to trauma events has been previously reported. For example, a FEM-TBI study parametrically evaluated the effect of human brain size in intracranial stresses during a direct impact and found that they were inversely proportionate [47]. The authors suggested that variations in brain size should be considered in the development of brain injury criteria and TBI thresholds [47]. Another study showed that applying the same impact kinematics to head FEMs with different sizes, or the same size but different shapes, resulted in different peaks and distributions of strain, especially in the corpus callosum [48]. The peaks and distributions of strain in the brain were shown to be related to the severity and distribution of TBI pathology, and thus the brain/head size, shape, and structural variations should be considered, and correctly modeled, when using brain FEMs to study TBI. However, despite recent recognition of sex variations in TBI vulnerability and clinical outcomes, the differences observed in brain structure, shape, and volume between females and males, and the importance of these parameters on the FEM simulation results, as discussed above, current brain FEMs, which usually are used to develop tissue injury thresholds and helmet standards, have been mainly developed based on a single or population-average adult male brain [49 51]. Therefore, the outcomes and findings of FEM-based research, the effectiveness of current protection and prevention strategies, and the accuracy of TBI risk assessments are biased towards males.

To take a step toward addressing these important sex-specific research needs and knowledge gaps, and to provide a foundation for development of sex-based FEMs of the human head, our present study aimed to 1) identify and characterize volumetric and structural differences between male and female brains; and 2) develop sex-specific brain templates that are most representative of their target groups. In the first part of this paper, we provide a detailed statistical information on the sex-based structural differences of human brain using a large dataset of female and male brain MRIs. In this part, volumetric analyses on different regions and sub-regions of the brain, as well as a cortical thickness analysis for male and female groups were performed. Moreover, insight into the sex variation in the fractional volume of different brain regions and sub-regions was provided by normalizing these volumes with respect to the TBV of each subject. Finally, multiple statistical tests were performed to determine significant differences between the parameters that were studied. The second part of this study was focused on generation of nonlinear brain templates for female, male, and mixed population. Thereafter, subcortical segmentation was performed on the developed templates and their corresponding values were compared with the population-based average values. Finally, the sex-specificity of each template, which determines how well each template represents its target group, was evaluated by nonlinear registration of a new set of female and male test subjects to the developed female-, male-, and mixed-population templates.

# Methodology

#### Data collection

For this study, 1330 brain T1 MRI images of healthy adults within the age range of 19 41, including 609 male and 721 female subjects were gathered. These images were acquired from different sources as explained in the following. T1 MRI images of 35 subjects, including 19 female and 16 male subjects, were acquired from the Emory University which approved by their local institution and informed consent acquired from patients [52]. An additional 35 MRI images were acquired from

Designed Database of MR Brain Images of Healthy Volunteers [53], consisting of 16 female and 19 male healthy subjects. 1113 brain T1 MRI images were taken from the HCP1200 dataset (Human Connectome Project) [21], of which 606 and 507 images corresponded to female subjects and male subjects, respectively. Finally, a part of the OASIS1 dataset [54], comprising 80 female and 67 male subjects within the selected age range of this study, were used in the accumulated final dataset. The schematic of the collected dataset with the age breakdown details can be seen in Fig. 1. The subject age was provided in five age ranges including 19 21, 22 25, 26 30, 31 35, and 36 41 years due to the fact that the exact age of subjects were not available in the HCP1200 dataset, and the age range was given there alternatively.

#### Brain subcortical segmentation

The FreeSurfer software (version 7.1.1) [17] was used for creating the brain masks and performing the subcortical brain segmentation of T1 MRI images. Here, the important steps involved in FreeSurfer segmentation pipeline, also known as image reconstruction will be explained. In the first step, the non-parametric non-uniform intensity normalization (N3) algorithm was applied to the head T1 MRI images, to correct any non-homogeneity of pixel intensities among the images because they were obtained from different resources and the pixel intensity range varied from one image to another. This step provides a consistent pixel intensity value for a certain tissue throughout the entire T1 MRI images [55]. In this step, the voxel-wise normalization was specified to have a mean intensity value of 110 for the corresponding estimated WM tissue. The Talairach coordinates were then used to register the image volume to the MNI305 atlas [56]. Subsequently, brain masks were generated by stripping the skull, meningeal, and other non-brain tissue, and removing the neck from the MRI images. Then, the registration of the brain masks to the Gaussian Classifier Atlas (GCA) [57] was performed, completing the brain segmentation workflow. The autorecon pipeline of the FreeSurfer package was used for performing the mentioned operations. We have randomly selected images from the reconstructed images to check for the quality of the segmentations. Moreover, we have used the pial surface modification in FreeSurfer for random 10 subjects with the available T2 image and since the difference in segmentations were found to be negligible (less than 1% for most of the regions), this process was skipped for other images in the dataset. The final generated brain masks for all data had the size of 256 256 256 with a voxel size of 1.0 mm 1.0 mm. 1.0 mm. Following brain segmentation, the volumes of different regions of the brain were calculated and the average GM cortical thickness estimated by determining the pial surface and WM segmentation. Upon the completion of these steps, the TBV, the average cortical GM thickness (Cort Thi), and the volume of 19 regions/subregions in the brain were calculated. These 19 regions with their corresponding acronym used in this manuscript are provided in Table 1. The regions 1 13 specified in Table 1, were calculated after merging the right and left hemisphere subregions. The CC region was merged from five subregions including the posterior, mid-posterior, central, mid-anterior, and anterior subregions of CC. The results of the right and left subregions of region 1 13 and five subregions of CC (total of 31 regions) are provided in the supplementary materials of this paper. Then, the Mann-Whitney test was employed to identify any significant sex-based structural differences with the probability level set to p = 0.05 for all analyses.

# Template generation

Using the brain masks generated from the FreeSurfer in the reconstruction step, female and male brain templates were generated for this study from 500 female and 500 male subjects randomly selected from the accumulated dataset of 1330 individuals (see Fig. 1). The mixed-population template was generated using 250 female and 250 male subjects that were randomly selected from the same accumulated

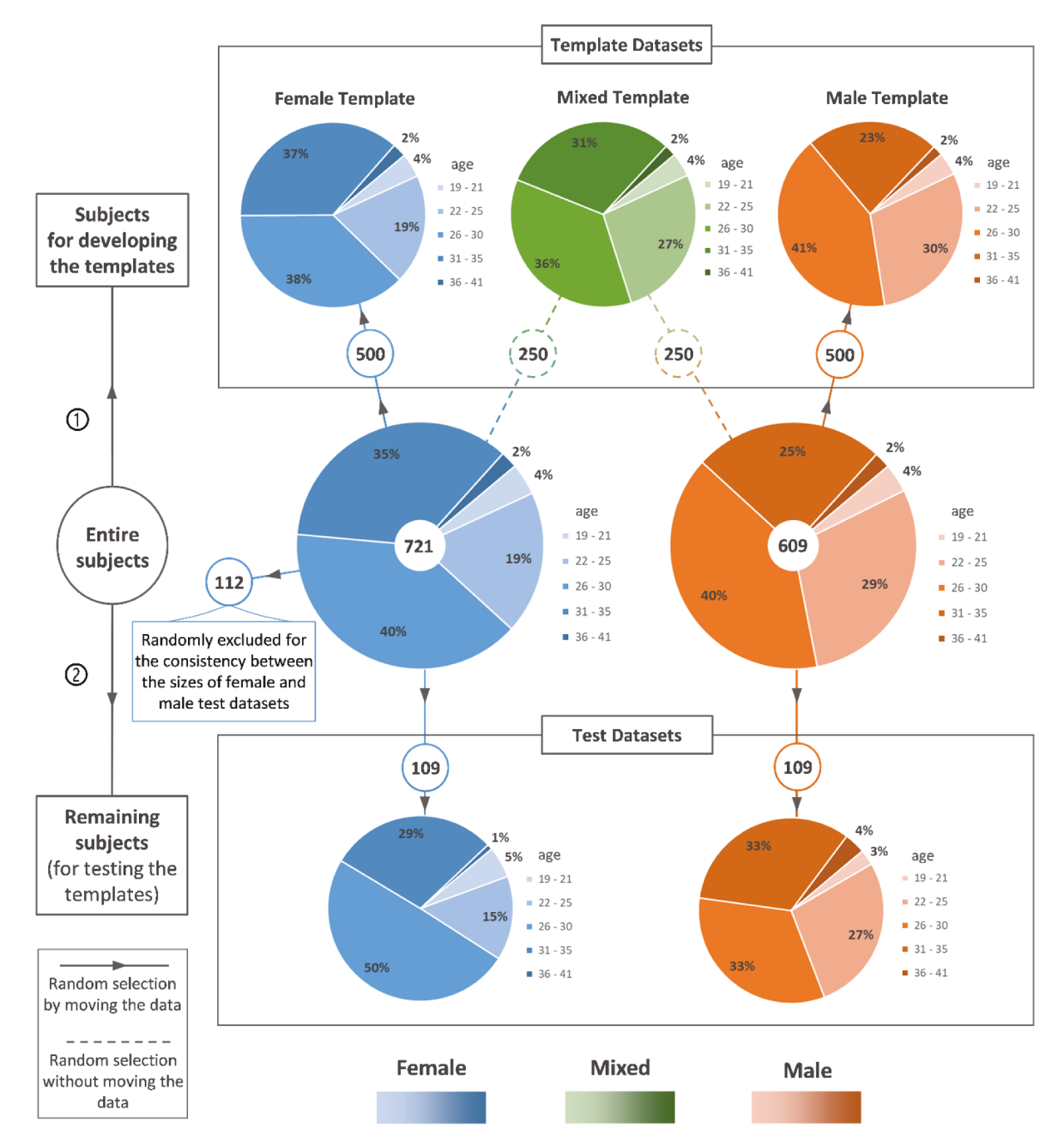


Fig. 1. A detailed breakdown on the brain T1 MRI image dataset and the sampling process for testing and template generation, based on age and sex.

dataset. As can be inferred, the same sample size (n=500) was used for generating each of these three templates to ensure that the sample size would not be a factor in any variations that may be found between these templates. The sample size of 500 was selected to ensure that the constructed brain templates is not affected by the sample size as the brain template variability showed to be reduced substantially after 200 images and reach a plateau at  $\geq$ 400 sample size [58]. The remaining images not used in the template generation process were used fully or partially as test samples for cross-validation of sex-specificity, as discussed in the next section (see Fig. 1 for details).

The "antsMultivariateTemplateConstruction2" module from ANTs (version 2.3.5) [18] was used to generate the female, male, and mixed-population nonlinear templates. The symmetric image normalization (SyN) method was used for the transformation and registration within that module. This transformation includes rigid, affine, and

nonlinear warping for image registrations. The registration steps in the SyN transformation were set as  $100\times70\times50\times20$  [18]. First, an initial template  $(T_0)$  was generated by rigidly aligning the images of all subjects to an arbitrary image in the dataset and subsequently averaging them. In the next step, all the images were registered to the  $T_0$  template and the  $T_1$  template was generated through averaging of all the nonlinearly registered images which marks the end of the first iteration. In the subsequent iterations, the template  $T_i$  was generated through nonlinear registration of the images into the template  $T_{i-1}$  and averaging them. It should be noted that Laplacian sharpening was used to increase the visibility of the generated intermediate and the final templates. The intermediate templates generated at each step were compared to their adjacent iteration template using correlation ratio and the relative convergence threshold was set as 0.001 as a stopping criterion. The correlation ratio, which determines the level of similarity between two

Brain Multiphysics 4 (2023) 100077

**Table 1**The brain regions or parameters studied in this manuscript and their corresponding acronym used throughout the manuscript.

#	Brain region/parameter	Acronym/term in this paper			
	Total brain volume	TBV			
	Cortical thickness	Cort Thi			
1	Cerebellum white matter	Cblm-WM			
2	Cerebellum gray matter/cortex	Cblm-GM			
3	Cerebral white matter	Cbral-WM			
4	Hippocampus	Hipp			
5	Thalamus	Thalamus			
6	Lateral ventricle	Lat Vent			
7	Pallidum	Pallidum			
8	Amygdala	Amygdala			
9	Cortical gray matter	Cor GM			
10	Accumbens area	Acc			
11	Caudate	Caudate			
12	Putamen	Putamen			
13	Subcortical gray matter	Sub-Cor GM			
14	Optic chiasm	Optic-Chi			
15	Cerebrospinal Fluid	CSF			
16	Third Ventricle	3rd Vent			
17	Fourth Ventricle	4th Vent			
18	Corpus callosum	CC			
19	Brain stem	Brain stem			

images is calculated as the following:

where  $I_{1i}$  and  $I_{2i}$  denotes the intensity of the voxel i from the flattened vectors I of the first and second image matrices, respectively. The  $m_k$  and  $s_k$  represents the mean and the standard deviation of pixel intensities in image k. The two images were assumed to have same dimension and the total number of pixels is denoted by N.

# Template sex-specificity evaluation

In this section, several steps that were taken, and different metrics that were used to evaluate how the female, male, and mixed-population brain templates were representative of their target populations, will be explained. This evaluation process will be called sex-specificity assessment throughout this paper. To that end, the brain images of the remaining 109 male dataset that were not used in the development of the generated templates were selected as the test dataset. To minimize the effect of the differences in the number of test subjects throughout the assessment process, we randomly selected 109 female images out of the remaining 221 female images that were not used for the template generation. For the graphic illustration of the sampling and the dataset details, refer to Fig. 1. Next, the female and male test datasets were nonlinearly registered to the generated templates using the SyN method in ANTs to find the corresponding voxel-wise deformation fields. To measure the level of changes that test images were undergone during the registration process, the determinant of the Jacobian of the deformation field for a voxel (*i*, *j*, *k*) was calculated using the following equation:

(2)

The mean value of the logarithm of the Jacobian for each test registration batch was then calculated using the following formulation [58]:

where n denotes the number of subjects in the test, r specifies the region of the brain,  $N_r$  is the number of voxels in that region, and J denotes the

calculated Jacobian of the deformation field for the voxel t calculated from Eq. (2). The log transformation on the Jacobian determinant is shown to be imperative for evaluating morphometric changes [59]. The above formulation makes the  $J_r$  metric independent of the coordinate system (fixed or moving image) used to calculate the Jacobian. When the fixed image coordinate is used, the positive and negative log-value of the Jacobian indicates a voxel-wise contraction or expansion, respectively. Therefore, by summing the absolute values in the  $J_r$  formulation and averaging, both contractions and expansions contribute to the  $J_r$  calculation equally.

The first step toward the nonlinear SyN registration in ANTs is the linear affine registration, in which all the image voxels are similarly expanded or contracted. This linear registration globally changes the image and hence this linear manipulation of the image should be considered for evaluation of the sex-specificity of the templates in addition to the  $J_r$  metric which assess the non-linear manipulation. The linear changes experienced by the images of the test subjects during the registration to the template was calculated using the following formulation:

(4)

Where the matrix L in equation (4) is the 12-DOF affine linear transformation matrix. The n in Eq. (5) denotes the total number of test images used in the registration process. Moreover, the amount of linear scaling in different directions ( $S_x$ ,  $S_y$ , and  $S_z$  in cartesian coordinates corresponding to left-right (RL), inferior-superior (IS), and posterior-anterior (PA) directions) were found using avscale module in FSL (version 6.0.5) [60].

Linear transformation (L), non-linear manipulations ( $J_r$ ), and directional scaling values were calculated from the non-linear registration (SyN) of the selected 109 male and 109 female test subjects to the female, male, and mixed brain templates to study the sex-specificity of each template. The generated deformation field of the nonlinear registration was used for calculating the Jacobian of deformation field at each voxel of the test images. The affine transformation part of the SyN registration method was used for calculating the global and directional scaling values applied to each voxel of the reference test image.

# Results

In this section, we illustrate the values and population distributions of the parameters, including the total and regional brain volumes and average GM thickness, identified through the segmentation step, and present the results of statistical analyses performed on them. This section is broken down into three parts. In the first part, the volumetric values of different parts of the brain will be presented. Next, the nonlinear templates developed for different target groups will be presented. Finally, the sex-specificness evaluation of the templates will be discussed.

Comparison of overall and regional differences in male and female populations: absolute and proportional volumes

The first parameters compared between female and male brains were the TBV and the overall cortical or GM thickness (Fig. 2). These comparisons showed that the TBV values were greater in male subjects compared to the female population. The distribution of TBV was shown to be varying by sex, with wider distribution in males while the TBV values were more concentrated around the median for females. The

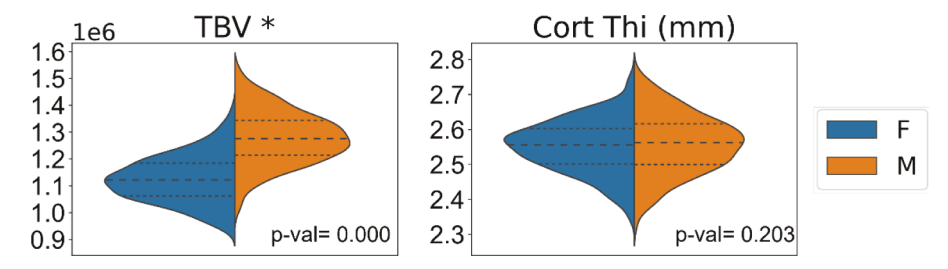


Fig. 2. Sex-based distribution and comparison of the total brain volume (mm<sup>3</sup>) and cortical thickness (mm). The asterisk \* represents significant differences.

cortical thickness, with an average of 2.557 mm and 2.548 mm for females and males, respectively, was not significantly different between these two populations (p=0.059). However, the distribution of cortical thickness in female and male populations is observable to be different, with males having a more elongated distribution, while the distribution in females was more concentrated in the middle of the violin plot (Fig. 2), meaning that the female population have near-median cortical thickness values.

Fig. 3 represents the sex-based distribution and comparison of absolute volumes for different regions of the brain. The absolute volumes of WM-related regions including CC, brain stem, Crblm WM, and Crbl WM showed significant differences in both mean and distribution between females and males with males having larger WM-related volumes compared to females. However, these sex differences were smaller in the CC region compared to the other three regions. The GM-related regions including cortical GM, subcortical GM, Crblm cortex, thalamus, and hippocampus also varied by sex, with the male population having larger regional volume on average compared to the female population. Caudate, putamen, and accumbens area which are mixed WM and GM were also found to be different between males and females. Looking at CSF, 3rd, 4th, and lateral ventricles, it can be inferred that they are significantly larger in males. Finally, amygdala, optic chiasm (Opt Chi), showed sex-based significant difference with the male subjects showing

greater values compared to females.

Although the sex variations were observed in the overall and regional brain volumes, it is not clear whether these differences are proportional to the TBV variations that exist between females and males or there are differences in the fraction of different brain regions with respect to the TBV. Therefore, in addition to the absolute volumes of the regions, the fractional volumes of the segmented regions with respect to the TBV were calculated for all the regions presented in Fig. 3 and the results are presented in Fig. 4. Table 2 provides the averages and standard deviations of the absolute regional and total brain volumes and the averages of the fractional regional volumes for females and males. Comparing the fractional regional volumes between all female and male datasets using Mann-Whitney test showed significant differences in all regions except CSF, cortical GM, and optic chiasm. The average percentage that female absolute and fractional volumes are larger (positive) or smaller (negative) than male brains are also calculated and provided in Table 2. The female-to-male percentage difference for each region was calculated by dividing the difference between female and male average volume for that region by the average of volume of that region in female population ((avg\_F-avg\_M)/avg\_F). Interestingly, the majority of the fractional regional volumes were larger in the female population than the male population except in the cerebral ventricular system (CSF, 3rd, 4th, and lateral ventricles), cerebral WM, and amygdala. The largest

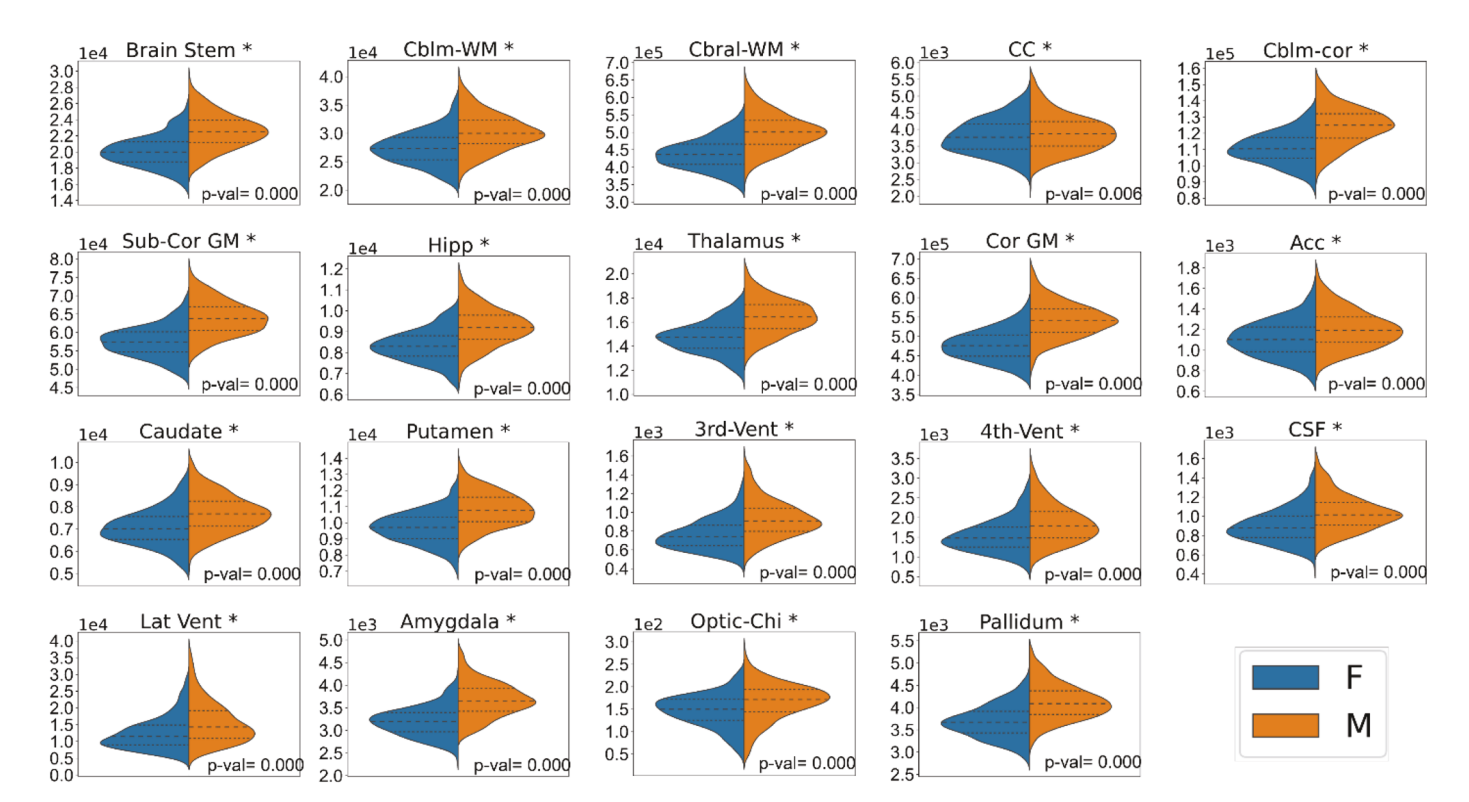


Fig. 3. Sex-based distribution and comparison of the volume of 19 regions of the brain for female (F) and male (M) subjects. The illustrated results are for the 500 F and 500 M subjects that were used in the process of generating female and male templates. The asterisk \* symbol denotes the statistically significant difference.

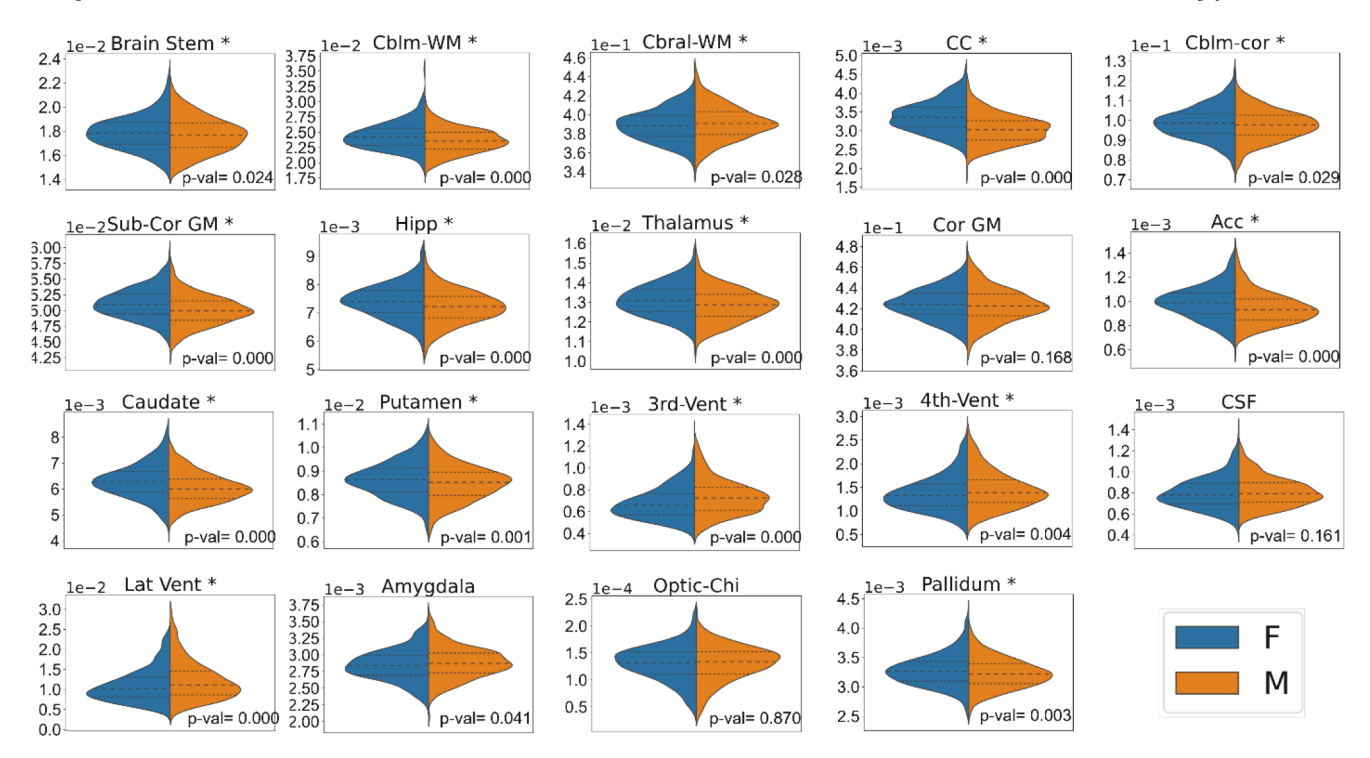


Fig. 4. Sex-based distribution and comparison of the fractional volume of 19 regions of the brain for female (F) and male (M) subjects normalized to each subject TBV value. The illustrated results are for the 500 F and 500 M subjects that were used in the process of generating female and male templates. The asterisk \* symbol denotes the statistically significant difference.

Table 2 Comparing the brain sex variations by providing the average (Avg) and standard deviation (SD) of the cortical thickness and the absolute (Abs) total (TBV) and regional brain volumes, the average of fractional regional (Frac) volumes, and the regional female-to-male percentage differences (Diff F&M% Abs and Diff F&M% Frac) for the female (n = 500) and male (n = 500) data sets.

Brain region	Avg F Abs	SD F Abs	Avg M Abs	SD M Abs	Avg F Frac	Avg M Frac	Diff F&M % Abs	Diff F&M % Frac
TBV	1,127,009	89,645	1,281,462	101,553				
Cort Thi	2.551	0.076	2.558	0.086				
Cblm-WM	27,513	3200	30,387	3562	0.024	0.024	-10.45	2.85
Cblm-cor	110,789	10,360	124,546	11,279	0.099	0.097	-12.42	1.15
Cbral-WM	439,008	44,411	502,644	52,474	0.389	0.392	-14.5	-0.68
Hipp	8321	762	9222	883	0.007	0.007	-10.83	2.57
Thalamus	14,750	1338	16,443	1431	0.013	0.013	-11.47	1.93
Lat Vent	12,795	5570	16,166	7236	0.011	0.013	-26.34	-11.5
Pallidum	3693	377	4130	395	0.003	0.003	-11.83	1.63
Amygdala	3210	342	3684	386	0.003	0.003	-14.75	-0.91
Cor GM	478,321	40,328	542,206	45,358	0.425	0.423	-13.36	0.29
Acc	1118	180	1210	188	0.001	0.001	-8.3	4.65
Caudate	7095	817	7736	861	0.006	0.006	-9.02	4.14
Putamen	9722	982	10,838	1052	0.009	0.008	-11.48	1.91
Sub-Cor GM	57,507	4195	63,909	4593	0.051	0.05	-11.13	2.25
Opt Chi	146	38	166	42	0	0	-13.26	0.26
CSF	906	197	1046	206	0.001	0.001	-15.37	-1.35
3rd-Vent	770	191	942	226	0.001	0.001	-22.42	-7.81
4th-Vent	1560	438	1864	541	0.001	0.001	-19.51	-5.14
CC	3800	530	3905	565	0.003	0.003	-2.77	9.63
Brain Stem	20,167	2005	22,620	2203	0.018	0.018	-12.17	1.34

average percentage differences in fractional regional volumes were observed in CC and lateral ventricle. The average of fractional CC volume showed to be about 10% larger in females than males and the average of fractional lateral ventricle volume showed to be 12% smaller in the female population. Other brain regions with larger average fractional values in females are bolded in the last column of Table 2. These results indicate that the regional differences between female and male brains are not proportional to the total brain volume differences and vary from one region to another.

# Developed sex-specific templates

In this section, the results of the subcortical segmentations on the male, female, and mixed-population brain templates generated in this study (Fig. 5) will be reported. Fig. 5 presents the multi-slice view of the female, male, and mixed brain template in axial, coronal, and sagittal planes. As the size of these templates vary, for the comparison purposes, the three slices shown in each view are placed at 25th, 50th, and 75th percentile of their length in their corresponding plane. As mentioned in the Methodology section, we used the

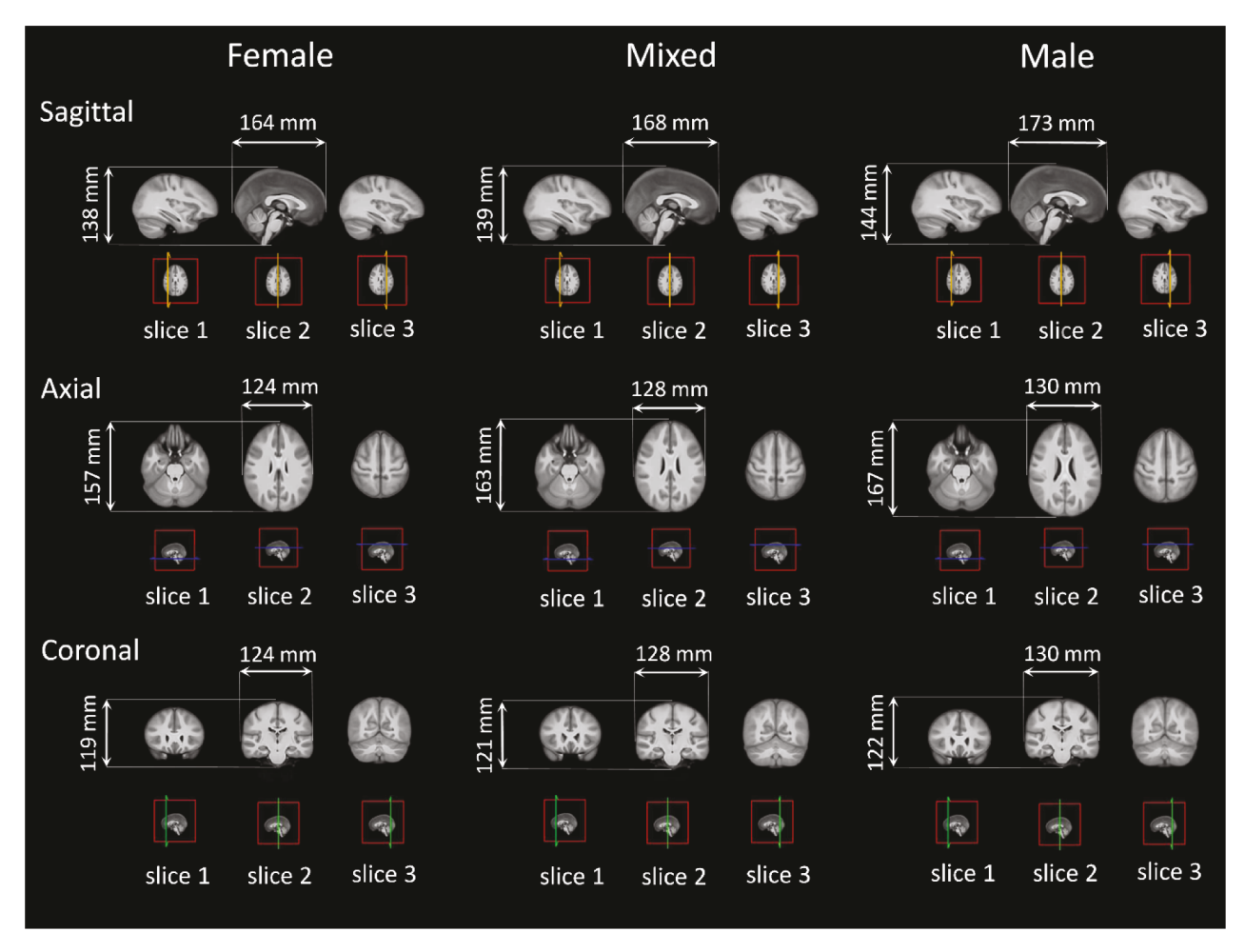
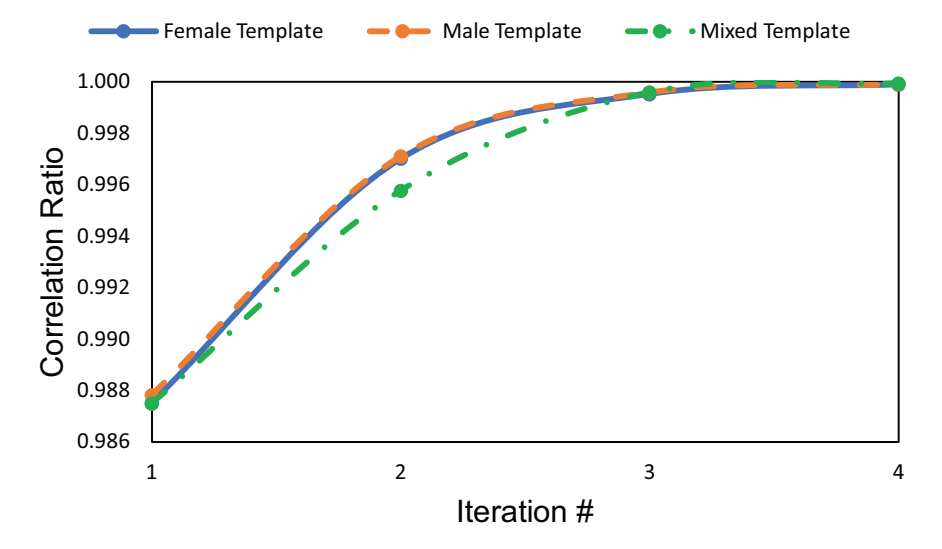


Fig. 5. The generated female, male, and mixed-population brain templates from T1 MRI images. Three brain slices (25th, 50th, and 75th percentile of the template length) with similar relative position across templates are shown for sagittal, axial, and coronal views.

"antsMultivariateTemplateConstruction2" script for generating the templates, based on the similarity of the generated templates in consecutive iterations and the relative convergence ratio of 0.001, it took 4 iterations for all the templates to be generated. The correlation metric variation between consecutive templates with respect to the

number of iterations are shown in Fig. 6. The correlation metric at iteration i shows the correlation metric between the templates generated at iteration i and iteration i - 1. It should be noted that iteration 0 refers to the linear average of all images in the dataset after the initial rigid alignment. As can be seen from Fig. 6, a plateau is starting to form at the



**Fig. 6.** The similarity of the templates generated in consecutive iterations measured through the correlation ratio metric. Iteration i (x-axis) denotes the similarity of the templates generated at iterations i and i-1.

fourth iteration and moreover, the correlation ratio gets very close to 1.0, which indicates a high level of similarity between the template generated at the iterations 3 and 4 and thus decided that no further iteration in the process of template generation was necessary after the 4th iteration.

The segmentation results for the total brain and subcortical volumes of the female, male, and mixed-population templates, as reconstructed in FreeSurfer, are given in Table 3. The average and standard deviations of the TBV and regional volumes for the female and male populations are given in Table 2 and values for the mixed population are provided in Table 3. The percentage differences between the volumes of the segmented regions in the representative templates and the average of the dataset populations (500 females and 500 males) are also provided in Table 2. As can be seen from Table 3, the differences between the population targeted templates and the average of the populations were less than 10% for the majority of the segmented regions, particularly for the female and male templates, indicating that these templates are representative of the average of their populations. However, for some regions, such as cerebellum WM and lateral ventricle, these differences were higher. This difference was found to be high in all three templates for the cortical thickness ( $\sim$ 20%) as well. In addition, these differences were noticed to be larger in mixed populations compared to the female or male template/population, which also indicates the advantages of developing sex-specific templates.

### Sex-based specificness of templates

In this section, the results of the sex-specificness analysis of the developed templates will be provided. As mentioned in the method section, 109 male and 109 female test subjects were nonlinearly registered to the three developed templates using the SyN transformation in ANTs package. As the first part of the SyN transformation is a linear affine registration, first the amount of linear scaling in different directions for all the test subjects was calculated. Fig. 7 represents the linear scaling value in different directions/anatomical planes (denoted by x, y, and z here) for the test female and test male subjects, respectively. The  $S_x$ ,  $S_y$ , and  $S_z$  are the amount of linear scaling performed along the left-right (RL), inferior-superior (IS), and posterior-anterior (PA) axes, respectively. The abbreviations F, M, and X refer to female, male, and mixed population. For example, F2X means registration of female test subjects to the mixed template. As can be seen from those

figures, the female test subjects needed expansion when linearly registered to the mixed and male templates, in accordance with our expectation of male and female size of the brain (Tables 2 and 3). The scaling factors were slightly different in each direction, with average 4.9%, 5.8%, and 5.6% expansions in IS, PA, and RL directions when females were registered to male template. As expected, the shrinkage in size (scaling 1) was noticed for male test subjects in their registration to the female template. The averages of linear scaling values are reported in Table 4.

For the nonlinear deformation, the logarithm of the Jacobian  $(J_r)$  for registration of each female (or male) test subject to the female (or male), male (or female), and mixed population brain templates were calculated for all voxels. Fig. 8 represents the visualization of the Jacobian of the deformation field averaged over the male and female test subjects registered to the female, mixed, and male templates. In the ANTs package, the Jacobian of the deformation field is calculated in the fixed image coordinate space (template) and therefore, the positive values (warm colors) indicate shrinkage in the voxel and the negative values (cold colors) indicate an expansion in the voxel. Black color represents no deformation in the corresponding voxel. One pattern that can be seen in Fig. 8 for both female and male test sets is that the shrinkage is happening mostly at the outer parts of the brain, while the inner part mostly goes through expansion. More importantly, F2F and M2M showed more black areas than F2M or M2F, meaning that the images were underwent no/lower deformations when registered to their own sex-specific brain template. Table 4 presents the overall and regional  $J_r$ values of the female test subjects (n 109) when they were nonlinearly registered to the female, male, and mixed brain templates abbreviated as F2F, F2M, and F2X, respectively. Similar analyses were performed for male test subjects (n 109) by the registration of the test male subjects to the male (M2M), mixed population (M2X), and female (M2F) brain templates, respectively.

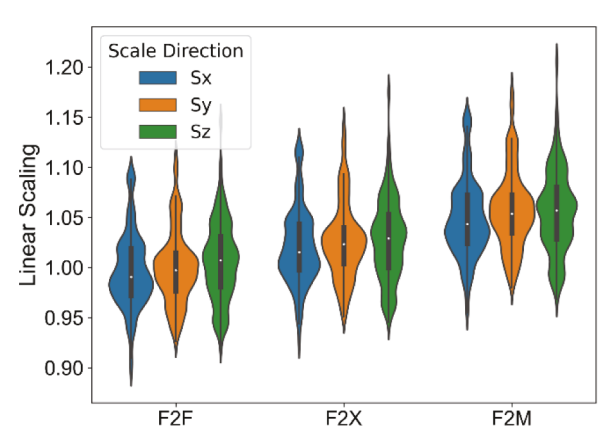
# Discussion

All reported volumetric parameters for the whole and different regions of the brain were found to be significantly greater in males compared to females emphasizing on the inherent sex-based differences in human brain structure. These findings are aligned with several previous studies [9 12]. For example, similar to out findings, Peters et al. [13] found TBV to be greater in males compared to females.

Table 3

Comparing the total (TBV) and regional volumetric values of the representative female (F), male (M), and mixed (X) population templates generated in this study and the average (AVG) absolute volumetric values of the corresponding populations, dnoted with Diff Temp vs Avg% for F, M, and X. The average absolute regional volumetric values for female and male populations are provided in Table 1 and those values for mixed populations are provided in this table.

Brain region	Template F	Diff temp vs Avg% F	Template M	Diff temp vs Avg%M	Template X	Diff temp vs Avg% X	Avg X Abs	SD X Abs
TBV	1,115,337	1.05	1,276,624	0.38	1,138,741	5.45	1,200,781	0.09
Cort Thi	3.121	18.26	3.15281	18.87	3.286	22.4	2.55	0.08
Cblm-WM	34,739	20.8	39,652	23.37	36,399	20.48	28,945	0.12
Cblm-cor	105,215	5.3	120,072	3.73	101,877	15.64	117,814	0.11
Cbral WM	411,193	6.76	479,453	4.84	424,261	10.61	469,290	0.11
Hipp	7769	7.11	8416	9.58	7589	15.11	8736	0.1
Thalamus	14,634	0.79	17,696	7.08	15,914	2.73	15,480	0.1
Lat Vent	12,279	4.2	16,498	2.01	13,453	6.67	14,350	0.48
Pallidum	3778	2.25	3980	3.77	4332	10.09	3895	0.1
Amygdala	3157	1.68	3708	0.65	3225	5.86	3414	0.12
Cor GM	492,699	2.92	554,839	2.28	502,331	1.25	508,602	0.1
Acc	1201	6.91	1237	2.18	1111	5.04	1167	0.17
Caudate	6041	17.45	7791	0.71	6683	10.88	7410	0.12
Putamen	8410	15.6	9689	11.86	8792	16.79	10,268	0.11
Sub-cor GM	56,047	2.6	62,443	2.35	57,539	5.07	60,458	0.08
Opt chi	148	1.35	113	46.9	101	53.47	155	0.26
CSF	899	0.78	1039	0.67	921	4.89	966	0.23
3rd-Vent	749	2.8	936	0.64	800	6.38	851	0.24
4th Vent	1530	1.96	1813	2.81	1792	5.08	1701	0.3
CC	3912	2.86	4043	3.41	4066	5.83	3829	0.13
Brain Stem	19,293	4.53	21,683	4.32	19,560	8.8	21,281	0.11



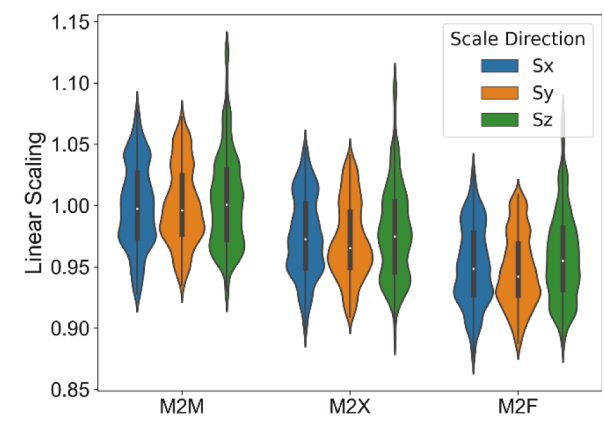


Fig. 7. The linear scaling value in different directions for registration of the 109 test female (F) and 109 test male (M) subjects to the developed female (2F), mixed (2X), and male (2 M) templates.

#### Table 4

The linear scale values  $(S_x, S_y, S_z, \bar{L})$  and the jacobian metric  $(\bar{J_r})$ , representating non-linear deformation after linear transformation, obtained from nonlinear registration of the female and male test subjects to the developed sex-specific templates are provided. F2F, F2M, and F2X denotes the results of the registration of female test subjects to the female, mixed, and male brain templates respectively. M2M, M2X, M2F indicates the registration of test male subjects to the male, mixed, and female brain templates, respectively.

Parameter/Region $(\bar{J}_r)$	F2F	F2X	F2M	M2M	M2X	M2F
$S_{x}$	0.997	1.021	1.049	1.000	0.975	0.951
$S_{y}$	1.000	1.027	1.058	1.000	0.971	0.947
$S_z$	1.006	1.028	1.056	1.004	0.978	0.958
$ar{L}$	0.061	0.081	0.150	0.067	0.102	0.155
Brain- Total	0.155	0.161	0.165	0.161	0.158	0.154
Cblm-Cor	0.154	0.161	0.166	0.160	0.156	0.152
Crbl-WM	0.158	0.160	0.163	0.162	0.162	0.161
Hipp	0.136	0.141	0.143	0.143	0.147	0.148
Thalamus	0.139	0.135	0.131	0.152	0.170	0.179
Lat Vent	0.214	0.222	0.226	0.217	0.199	0.189
Pallidum	0.100	0.100	0.104	0.104	0.119	0.131
Amygdala	0.135	0.137	0.138	0.124	0.125	0.124
Cor GM	0.158	0.166	0.172	0.164	0.157	0.149
Acc	0.112	0.113	0.115	0.116	0.128	0.137
Caudate	0.150	0.150	0.146	0.150	0.151	0.153
Putamen	0.125	0.124	0.127	0.129	0.132	0.139
Opt Chi	0.105	0.114	0.137	0.125	0.118	0.114
CSF	0.173	0.174	0.170	0.178	0.184	0.184
3rd Vent	0.138	0.142	0.143	0.153	0.150	0.154
4th Vent	0.151	0.153	0.153	0.148	0.154	0.155
CC	0.171	0.172	0.177	0.169	0.174	0.180
Brain Stem	0.115	0.117	0.119	0.114	0.117	0.120

Additionally, when comparing the absolute volume values of different brain regions between males and females, we observed a similar pattern, which was consistent with the meta-analyses conducted by Ruigrok et al. [12] across different brain regions. These meta-analyses also reported high sex differences in total gray matter, white matter, and cerebellum, with males exhibiting larger absolute volumes, which corroborates our findings. Regarding the relative volumetric parameters, the review study by Cosgrove et al. [10] reported that the volume of amygdala relative to the total brain volume was larger in men, while women tend to have a larger caudate and hippocampus. Similar findings can be observed in this study (Table 3). Considering such sex-specific structural differences, the other question that needed to be answered was whether simple uniform linear scaling of the male brain can accurately represent the female brain structure or not. Per Table 3, the average male to female ratio of the volumetric parameters were not the same for all brain regions, but varied by brain region, ranging from 1.03 for corpus callosum up to 1.27 for the lateral ventricle. These regional ratios were also different from the average male-to-female TBV ratio (1.14). These

results indicate that the sex-based structural differences and sex variations in regional brain/head size cannot be addressed by global/uniform scaling. The fractional regional volumes, which were calculated by normalizing the volume of the segmented regions to TBV and reported in Table 2, also showed that the difference in overall brain size is not the only determining factor in the sex-based variations in the brain. Contrary to what was seen for the actual/absolute values, the fractional volumes of many regions were found to be greater in females than males, notably in corpus callosum, subcortical GM, hippocampus, brain stem, cerebellum WM, cerebellum cortex, thalamus, caudate, and accumbens area. The higher fractional volume of the subcortical GM and cortical GM is in agreement with the findings of Luders et al. [11] in which TBV matched groups of females (N = 24) and males (N = 24) were compared. However, in that study, the TBV matched volume of WM was reported to be higher for males compared to females which is different compared to our findings. The difference could be rooted at the smaller sample size of dataset (N = 48 in their study vs N = 1000 herein), different age ranges (18-70 years in that study vs 18-41 herein), and different approach (TBV matched in that study vs fractional or ratio to TBV herein) used in [11] compared to this study. The variations in the fractional regional volumes and their corresponding female-to-male percentage differences (Table 3) confirm that the sex-based structural variations in the brain are not just proportional to the sex differences in TBV and cannot be addressed by uniform and global scaling. Moreover, some of the parameters were found to be still significantly different after being normalized with respect to the TBV.

As mentioned in the introduction section, the sex-based structural differences could be a deterministic factor for FEM simulations that are used to draw cross-sex conclusions regarding TBI. Therefore, the sexbased variations in the absolute overall and regional volumes that we found suggest that the FE model based on a single or averaged population male cannot properly mimic the brain responses to head impact exposures in females. We further assessed the global scaling concepts between female and male brains. To that end, we linearly registered the test male and female subjects to the three templates, as discussed in the Methodology section and the results are presented in Fig. 7. As expected, the average of linear scaling of the female test subjects to the female template were closer to 1 while they were greater than 1 when registered to the mixed or male brain templates. As half of the subjects in the mixed template were from the female population, the scaling value for "F2X" category lay between the "F2F" and "F2M", as expected. The same pattern can be seen for the male test subjects. As can be seen in Fig. 7, the linear scaling value varies in different anatomical directions. For example, the average scaling factors for female to male brain were 1.049, 1.058, and 1.056 along the x, y, z axes. These values are also different from the factors from a uniform TBV-based scaling technique

[37,61] (
$$Sx = Sy = Sz = \left(\frac{TBV - Avg - M}{TBV - Avg - F}\right)^{\frac{1}{3}} = 1.046$$
 in all 3 directions) which

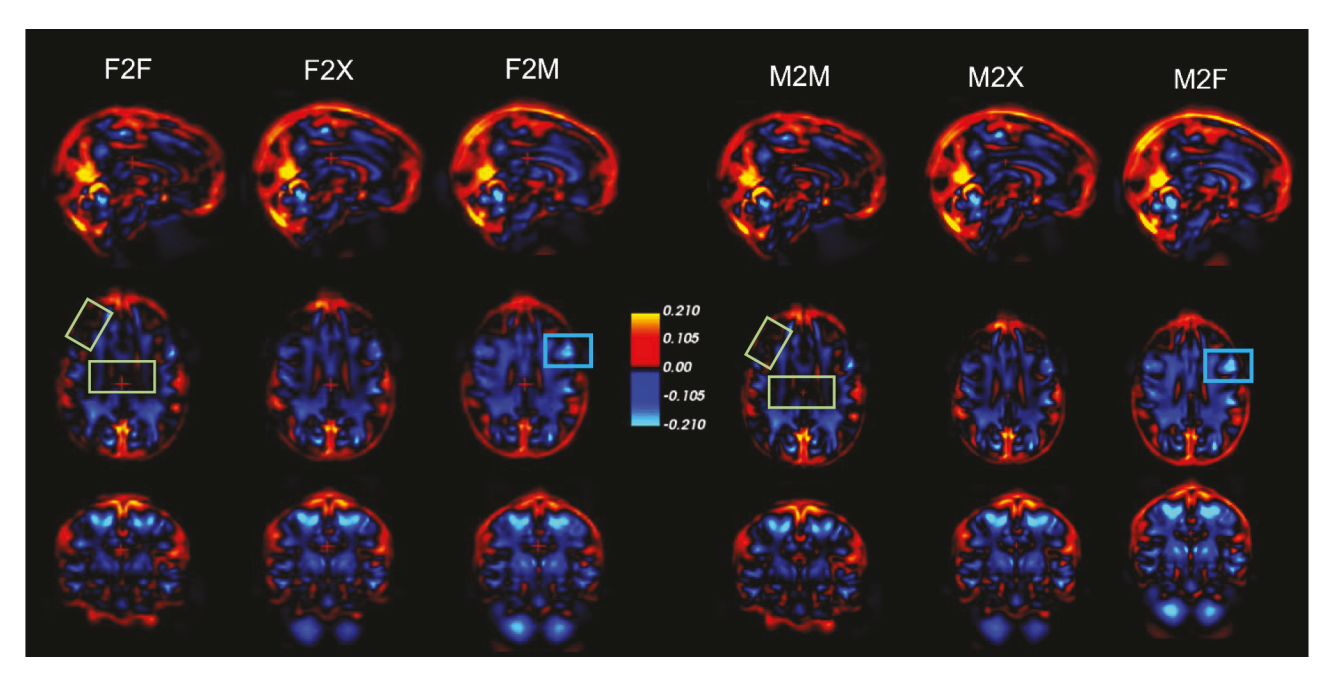


Fig. 8. The average of the Jacobian of the deformation field calculated from nonlinear registration of the test subjects into different templates. The boxes on F2F and M2M images show black areas for the deformation field which mean no/minimal manipulation throughout the registration process. The boxes on F2M and M2F (cyan color) images show areas with light blue for the deformation field which illustrate high expansion in those areas throughout the registration process.

is a common scaling approach in the FE-TBI studies. Therefore, while we do not recommend linear scaling for male to female brain FEM translation based on the results presented in this paper, such scaling methods would benefit from non-uniform directional-dependent scaling  $(S_x, S_y, \text{ and } S_z)$ , as provided in Table 4, if decided to do linear scaling for FEMs.

To evaluate the suitability of developed sex-specific templates, test female and male images were nonlinearly registered to the three female, male, and mixed templates and the mean regional Jacobian metric  $(\bar{J}_r)$ were calculated. These values which are provided in Fig. 8 and Table 4, determine the level of voxel and regional manipulations (expansion or shrinkage) that the brain undergoes in ANTs SyN nonlinear registration after the completion of linear registration. From Table 4, it can be inferred that the Jacobian metric value for all the brain regions, with the exception of thalamus, caudate, and CSF, are either equal or smaller in the F2F registrations compared to F2X or F2M registrations. This confirms that beyond the apparent change of size in female template compared to male or mixed-population templates, the local regionalwise change is also different. This finding reiterates the importance of developing a female-specific brain model. Comparing the M2M and M2X values in Table 4, this pattern becomes less dominant. While many of the regions show equal or smaller values in M2M compared to M2X, there are some regions that do not follow this pattern. Moreover, compared to the female test subjects, we can see more regions that are equal in M2M and M2X (comparative to F2F and F2X). It should be noted that we have used a balanced number of male and female subjects for creating the mixed brain template to avoid any sex-based biasedness in the final mixed-population template. Therefore, these results may be explained by the wider range of (long-tailed) distributions observed in the violin plots for the male population. Looking into Fig. 8, it is apparent that the distribution and intensity of voxel-wise deformation is not similar when test subjects are registered to different templates. As an example, looking into F2F subjects average Jacobian, reveals more black area (marked by a green box) which is corresponding to close to zero deformation compared to other groups including F2X and F2M. Another example is how high expansion is seen in the left cortical WM/GM area in the M2F test subjects as indicated by intense blue color marked by a cyan box in the figure. All the points discussed above, further emphasize the importance of developing the female-specific brain template and FE model.

From the brain FEM perspective, based on the published FEM simulations performed for TBI analysis, CC and thalamus were reported to experience the highest shear stress and principal strain due to TBIinducing incidents [62]. Simulations with non-sex-specific FEMs indicated that the maximum principal strain of 0.074 in corpus callosum would lead to 50% chance of concussion [43]. Another question to be answered in the future is whether these findings would remain valid if sex specific FEMs are used, especially since the absolute and fractional/relative sizes of the corpus callosum and thalamus were shown to differ between females and males in this study. Another important question that needs to be explored is if, and how much, the fractional volumes of important regions in TBI, such as CC, thalamus, and brain stem would affect the susceptibility of female or male brains to damage due to impact/trauma-induced incidents. The summation of the points discussed in this section adds to the idea that valid cross-sex FE simulations require sex-specific human brain FEMs to be developed. Such brain FEMs need sex-specific brain templates in their development process.

The sex variations that we explored and found in the brain structures in this study can provide valuable information beyond the FE modeling of TBI. For example, the fact that the volumes of the CSF and ventricles were found to be larger in males than females, not only in absolute volumes but also fractional volumes, may explain some of the variations that are reported in the literature between females and males in terms of susceptibility to TBI and post-TBI outcomes and healing process [30–34, 63,64]. For example, many sport-based TBI studies have shown that females have a higher rate of concussion, longer return to play, higher post-concussive symptom scores, and more prolonged symptoms than their male counterparts in comparable sports (e.g. in soccer, softball, baseball, and basketball) [33,34,63,65-67]. These sex variations in the brain susceptibility and post-TBI outcomes may be partially attributed to the larger absolute and fractional CSF and ventricles volumes of males than females. These CSF-based brain regions, which are larger in absolute and fractional volumes in males than females, act as cushioning and physical shock-absorbing components for the brain and are responsible for removing waste after trauma, and thus may differentially affect TBI risks and outcomes in females and males [68]. The information provided

in this study regarding variation in brain structure by sex may facilitate understanding of some baseline or post-TBI sex-based differences, such as in the cognitive and neuropsychological domains.

Another point to discuss is the segmentation process. The accuracy of volumetric analyses and subcortical segmentations performed in this study is limited to the accuracy of FreeSurfer software used in this study. There are studies that found discrepancies between the results of the FreeSurfer and the manual segmentation for some regions of the brain [69]. Therefore, although performing manual segmentation for such large datasets is not feasible, future studies can compare the results of FreeSurfer with other software for automatic segmentations such as FSL FIRST to provide more insights on the level of accuracy, similarities and/or discrepancies between different automatic segmentation software and their effects on the sex variation evaluation. Moreover, it should be noted that the segmentation process in the FreeSurfer reconstruction is based on linear and nonlinear registration of the processed brain images to the gaussian classifier atlas (GCA) which is not a sex-specific atlas. This could impose another limitation on the segmentation results reported in this study. We have shown that sex-based structural variations go beyond the scaling and the regional sex-based variations exist in the human brain, it emphasizes the need for developing sex-specific atlases to account for this variation. Upon the development of sex-specific atlases, which requires a manual labeling process that can be done by experts, it would be anticipated that we could have more accurate segmentation results that considers the intra-sex variations. While the creation of probabilistic atlases requires manual segmentation to be done for multiple subjects, subject-specific atlases can be developed using one image. Therefore, as the templates generated in this study were shown to be a good representative of their target population, they can be used as a reference single image for creating those single-subject-based atlases.

While this paper was focused on the sex-based structural variation of brain, and the selected age range were relatively narrow (19 41 years), the effect and contribution of age on the variations observed in the volumetric results in this study were also examined. To that end, MANOVA and linear regression analysis were performed in SPSS on the volumetric parameters considering sex and age (thw 5 age intervals as described in methodology section) as two contributing factors. While sex found to be a significant factor in all brain regions and age found to be significant factor in most of brain regions, the relative importance of sex was 99% for TBV and on average 85% for all brain regions while the relative importance of age was 1% for TBV and on average 15% for other brain regions. Among all brain regions studied, CC and accumbens area were the only ones in which the relative importance of age was more than sex. In summary, the sex was shown to be the primary factor contributing to the variations observed in this study between female and males within age range 19 41. Also, the age range was confirmed to be sufficiently narrow eliminating the need for developing age-based brain templates. The importance of the age factor for younger (age 19) and older (age 41) populations and development of age-specific templates for those age range can be studied in future invstigations. In addition, it should be noted that while this study was mostly focused on finding the sex-based differences in human brain structure and studied a relatively large population of females and males, it is essential to recognize that sex alone may not be the sole determining factor responsible for the observed differences. Other factors like gender, hormones, environment, ethnicity, etc. might have affected the observation. These other factors can also play a role in shaping the human (or animals) brain structure as demonstrated in previous studies [70,71].

Finally, this study examined the sex variations in many structural/anatomical brain features including the overall average cortical thickness, TBV; and 19 regional volumes in the paper as well as 31 subregional volumes in the supplementary materials. Future research may examine regional sex variations in the context of functional or structural connectivity [72,73], or for brain or subregion parcellation [74,75].

#### Conclusion

While all the brain regions studied herein were found to be, on average, larger in males than females, these differences are not proportional to the overall brain volume/size. The fraction composition of those regions within the brain, denoted by fractional regional volumes and calculated by dividing the volume of each region by the TBV, are not the same in male and female subjects. Apparently, the fractional regional volumes, on average, are greater in females than males in many regions such as corpus callosum, cerebellum WM, brain stem, hippocampus, subcortical GM, etc. The fractional regional volumes are greater in males than females in a few regions such CSF and ventricles. The CSF and ventricles have cushioning and waste removal roles in the brain, and thus their sex variations may affect risks and outcomes of TBI in females and males. These fractional volume analyses also suggested that the uniform and global linear scaling is not appropriate and accurate approach when we translate brain templates or brain FEMs between males and females to do sex-specific or cross-sex analysis and such analysis requires sex-specific brain templates and brain FEMs. Therefore, in this study, the nonlinear templates were developed for the female (500 subjects), male (500 subjects), and mixed populations (250 female and 250 male subjects). Although large variations were observed, even within the female and male populations, the sex-specific brain templates were shown to be closer to their targeted populations than the opposite-sex or mixed-sex templates. The sex-specific brain templates were shown to be the best representative of their constitutive populations and thus can be used in and positively contribute to different fields such as TBI, other brain diseases and disorders, brain FEM, brain biomechanics, neuroscience, neuroimaging, etc.

#### **Ethical statement**

All the human subject brain images used in this study are either from public open-access repositories or from the published studies which were in accordance with the standard guidelines.

#### **Declaration of Competing Interest**

The authors declare that they have no known competing financial interests or personal relationships that could have appeared to influence the work reported in this paper.

## Data availability

Data will be made available on request.

# Acknowledgements

This work was supported by the National Science Foundation (grant number of 2138719). The authors would like to thank Dr. Morteza Seidi for his helps on the brain template development process. The authors acknowledge the computational support received from the High-Performance Computing Center (ARC) at the University of Texas at San Antonio.

# Supplementary materials

Supplementary material associated with this article can be found, in the online version, at doi:10.1016/j.brain.2023.100077.

#### References

- Forde, N.J., et al., Sex differences in variability of brain structure across the lifespan. 2020. 30(10): p. 5420 5430.
- [2] J.B. Becker, et al., Sex Differences in the Brain: From Genes to Behavior, Oxford university press, 2007.

- [3] Azim, E., et al., Sex differences in brain activation elicited by humor. 2005. 102 (45): p. S754.
- [4] Douaud, G., et al., SARS-CoV-2 is associated with changes in brain structure in UK Biobank. 2022. 604(7907): p. 697 707.
- [5] Sparks, B., et al., Brain structural abnormalities in young children with autism spectrum disorder. 2002. 59(2): p. 184 192.
- [6] Zagorchev, L., et al., Differences in regional brain volumes two months and one year after mild traumatic brain injury. 2016. 33(1): p. 29–34.
- [7] Maas, A.I., et al., Traumatic brain injury: integrated approaches to improve prevention, clinical care, and research. 2017. 16(12): p. 987–1048.
- [8] Ji, S., et al., Use of brain biomechanical models for monitoring impact exposure in contact sports. 2022: p. 1 20.
- [9] Ritchie, S.J., et al., Sex differences in the adult human brain: evidence from 5216 UK biobank participants. 2018. 28(8): p. 2959 2975.
- [10] Cosgrove, K.P., C.M. Mazure, and J.K.J.B.p. Staley, Evolving knowledge of sex differences in brain structure, function, and chemistry. 2007. 62(8): p. 847–855.
- [11] Luders, E., et al., Why sex matters: brain size independent differences in gray matter distributions between men and women. 2009. 29(45): p. 14265 14270.
- [12] Ruigrok, A.N., et al., A meta-analysis of sex differences in human brain structure. 2014. 39: p. 34 50.
- [13] Peters, M., et al., Unsolved problems in comparing brain sizes in Homo sapiens. 1998. 37(2): p. 254 285.
- [14] Kodiweera, C., et al., Age effects and sex differences in human brain white matter of young to middle-aged adults: a DTI, NODDI, and q-space study. 2016. 128: p. 180, 192.
- [15] J.S. Allen, H. Damasio, T.J. Grabowski, Normal neuroanatomical variation in the human brain: an MRI-volumetric study, Am. J. Phys. Anthropol. 118 (4) (2002) 341 358
- [16] Tustison, N.J., et al., Large-scale evaluation of ANTs and FreeSurfer cortical thickness measurements. 2014. 99: p. 166 179.
- [17] Fischl, B.J.N., FreeSurfer. 2012. 62(2): p. 774 781.
- [18] Avants, B.B., et al., A reproducible evaluation of ANTs similarity metric performance in brain image registration. 2011. 54(3): p. 2033 2044.
- [19] Talairach, J.J.A.a.t.c.i., Co-planar stereotaxic atlas of the human brain-3dimensional proportional system. 1988.
- [20] Mazziotta, J., et al., A four-dimensional probabilistic atlas of the human brain. 2001. 8(5): p. 401 430.
- [21] Van Essen, D.C., et al., The WU-Minn human connectome project: an overview. 2013. 80: p. 62 79.
- [22] Amunts, K., et al., The human brain project: creating a European research infrastructure to decode the human brain. 2016. 92(3): p. 574–581.
- [23] Assaf, Y., et al., The CONNECT project: combining macro-and micro-structure. 2013. 80: p. 273 282.
- [24] Rorden, C., et al., Age-specific CT and MRI templates for spatial normalization.
- 2012. 61(4): p. 957 965.
  [25] Richards, J.E., et al., A database of age-appropriate average MRI templates. 2016.
- 124: p. 1254 1259.[26] Liang, P., et al., Construction of brain atlases based on a multi-center MRI dataset
- of 2020 Chinese adults. 2015. 5(1): p. 1 7.

  [27] C.A. Rao, et al., A series of five population-specific Indian brain templates and atlases spanning ages 6 60 years, Hum. Brain Mapp. 41 (18) (2020) 5164 5175.
- [28] Hutchinson, E.B., et al., Detection and distinction of mild brain injury effects in a ferret model using diffusion tensor MRI (DTI) and DTI-driven tensor-based morphometry (D-TBM), 2018. 12: p. 573.
- [29] Seidlitz, J., et al., A population MRI brain template and analysis tools for the macaque. 2018. 170: p. 121 131.
- [30] V.C. Merritt, C.R. Padgett, A.J. Jak, A systematic review of sex differences in concussion outcome: what do we know? Clin. Neuropsychol. 33 (6) (2019) 1016 1043.
- [31] Gupte, R., et al., Sex differences in traumatic brain injury: what we know and what we should know. 2019. 36(22): p. 3063–3091.
- [32] Henry, L.C., et al., Examining recovery trajectories after sport-related concussion with a multimodal clinical assessment approach. 2016. 78(2): p. 232 241.
- [33] Dave, U., et al., Systematic review and meta-analysis of sex-based differences for concussion incidence in soccer. 2021: p. 1 9.
- [34] Preiss-Farzanegan, S.J., et al., The relationship between gender and symptoms after sport-related mild traumatic brain injury. 2009. 1(3): p. 245–253.
- [35] Covassin, T., R. Moran, and R. Elbin, Sex differences in reported concussion injury rates and time loss from participation: an update of the National Collegiate Athletic Association Injury Surveillance Program from 2004 to 2005 through 2008 2009. J. Athl. Train., 2016. 51(3): p. 189 194.
- [36] T. Covassin, P. Schatz, C.B. Swanik, Sex differences in neuropsychological function and post-concussion symptoms of concussed collegiate athletes, Neurosurgery 61 (2) (2007) 345–351.
- [37] Hajiaghamemar, M., et al., Embedded axonal fiber tracts improve finite element model predictions of traumatic brain injury. 2020. 19(3): p. 1109 1130.
- [38] M. Ghajari, P.J. Hellyer, D.J. Sharp, Computational modelling of traumatic brain injury predicts the location of chronic traumatic encephalopathy pathology, Brain 140 (2) (2017) 333 343.
- [39] C. Giordano, S. Kleiven, Development of an unbiased validation protocol to assess the biofidelity of finite element head models used in prediction of traumatic brain injury, Stapp Car Crash J. 60 (2016) 363.
- [40] M. Hajiaghamemar, S.S. Margulies, Multi-scale white matter tract embedded brain finite element model predicts the location of traumatic diffuse axonal injury, J. Neurotrauma 38 (1) (2021) 144 157.

[41] Wu, T., et al., Evaluation of tissue-level brain injury metrics using species-specific simulations. 2021. 38(13): p. 1879 1888.

- [42] Miller, L.E., et al., Evaluation of brain response during head impact in youth athletes using an anatomically accurate finite element model. 2019. 36(10): p. 1561–1570.
- [43] C. Giordano, S. Kleiven, Evaluation of axonal strain as a predictor for mild traumatic brain injuries using finite element modeling, Stapp Car Crash J. 58 (14) (2014) 29 61.
- [44] C. Deck, R. Willinger, D. Baumgartner, Helmet optimisation based on head-helmet modelling, WIT Trans. Built Environ. (2003) 67.
- [45] W. Decker, et al., Development and multi-scale validation of a finite element football helmet model, Ann. Biomed. Eng. 48 (1) (2020) 258 270.
- [46] M. Dymek, M. Ptak, F.A. Fernandes, Design and virtual testing of American football helmets a review, Arch. Comput. Methods Eng. (2021) 1 13.
- [47] S. Kleiven, H. von Holst, Consequences of head size following trauma to the human head, J. Biomech. 35 (2) (2002) 153 160.
- [48] J. Ho, S. Kleiven, Can sulci protect the brain from traumatic injury?, in: J. Biomech., 42, 2009, pp. 2074 2080.
- [49] E.G. Takhounts, et al., On the Development of the SIMon Finite Element Head Model, SAE Technical Paper, 2003.
- [50] S. Kleiven, Finite Element Modeling of the Human Head, KTH, 2002.
- [51] Sahoo, D., C. Deck, and R.J.J.o.t.m.b.o.b.m. Willinger, Development and validation of an advanced anisotropic visco-hyperelastic human brain FE model. 2014. 33: p. 24–42.
- [52] Smith, J.L., et al., The vestibular neuromatrix: a proposed, expanded vestibular network from graph theory in post-concussive vestibular dysfunction. 2022. 43(5): p. 1501 1518.
- [53] Bullitt, E., et al., Vessel tortuosity and brain tumor malignancy: a blinded study1. 2005. 12(10): p. 1232 1240.
- [54] Marcus, D.S., et al., Open access series of imaging studies (OASIS): cross-sectional MRI data in young, middle aged, nondemented, and demented older adults. 2007. 19(9): p. 1498 1507.
- [55] Belaroussi, B., et al., Intensity non-uniformity correction in MRI: existing methods and their validation. 2006. 10(2): p. 234 246.
- [56] Evans, A.C., et al., Brain templates and atlases. 2012. 62(2): p. 911 922.
- [57] B. Fischl, et al., Whole brain segmentation: automated labeling of neuroanatomical structures in the human brain, Neuron 33 (3) (2002) 341 355.
- [58] Yang, G., et al., Sample sizes and population differences in brain template construction. 2020. 206: p. 116318.
- [59] A.D. Leow, et al., Statistical properties of Jacobian maps and the realization of unbiased large-deformation nonlinear image registration, IEEE Trans. Med. Imaging 26 (6) (2007) 822 832.
- [60] Woolrich, M.W., et al., Bayesian analysis of neuroimaging data in FSL. 2009. 45(1): p. S173 S186.
- [61] C. Untaroiu, et al., Pedestrian kinematics investigation with finite element dummy model based on anthropometry scaling method, in: Proc. 20th Int. Technical Conf. Enhanced Safety of Vehicle, 2007.
- [62] M.J. Solomito, H. Reuman, D.H. Wang, Sex differences in concussion: a review of brain anatomy, function, and biomechanical response to impact, Brain Inj. 33 (2) (2019) 105–110.
- [63] Covassin, T., R. Moran, and R.J.J.o.a.t. Elbin, Sex differences in reported concussion injury rates and time loss from participation: an update of the National Collegiate Athletic Association Injury Surveillance Program from 2004 to 2005 through 2008 2009. 2016. 51(3): p. 189 194.
- [64] Covassin, T., P. Schatz, and C.B.J.N. Swanik, Sex differences in neuropsychological function and post-concussion symptoms of concussed collegiate athletes. 2007. 61 (2): p. 345–351.
- [65] Merritt, V.C., C.R. Padgett, and A.J.J.T.C.N. Jak, A systematic review of sex differences in concussion outcome: what do we know? 2019. 33(6): p. 1016 1043.
- [66] McGroarty, N.K., S.M. Brown, and M.K.J.O.j.o.s.m. Mulcahey, Sport-related concussion in female athletes: a systematic review. 2020. 8(7): p. 2325967120932306.
- [67] Cheng, J., et al., Sex-based differences in the incidence of sports-related concussion: systematic review and meta-analysis. 2019. 11(6): p. 486 491.
- [68] M. Toma, P.D. Nguyen, Fluid structure interaction analysis of cerebrospinal fluid with a comprehensive head model subject to a rapid acceleration and deceleration, Brain Inj. 32 (12) (2018) 1576–1584.
- [69] Schoemaker, D., et al., Hippocampus and amygdala volumes from magnetic resonance images in children: assessing accuracy of FreeSurfer and FSL against manual segmentation. 2016. 129: p. 1 14.
- [70] Grabowska, A.J.J.o.n.r., Sex on the brain: are gender-dependent structural and functional differences associated with behavior? 2017. 95(1 2): p. 200 212.
- [71] Corre, C., et al., Separate effects of sex hormones and sex chromosomes on brain structure and function revealed by high-resolution magnetic resonance imaging and spatial navigation assessment of the four core genotype mouse model. 2016. 221: p. 997 1016.
- [72] Balderston, N.L., et al., Functionally distinct amygdala subregions identified using DTI and high-resolution fMRI. 2015. 10(12): p. 1615 1622.
- [73] A.A. Alahmadi, Investigating the sub-regions of the superior parietal cortex using functional magnetic resonance imaging connectivity, Insights Imaging 12 (1) (2021) 1 12.
- [74] Fan, L., et al., The human brainnetome atlas: a new brain atlas based on connectional architecture. 2016. 26(8): p. 3508 3526.
- [75] Glasser, M.F., et al., A multi-modal parcellation of human cerebral cortex. 2016. 536(7615): p. 171 178.